Journal of Engineering Science and Technology
Vol. XX, No. Y (Year) PPP - QQQ

INVESTIGATION OF THERMOSOLUTAL CONVECTION IN A SIDE WALL HEATED AND SOLUTED CAVITY FILLED WITH A BINARY NANOFLUID

MOHAMED NAIMA[1,*], MOHAMMED ELMIR[1],
ELHADJ BENACHOUR[1], KHATIR NAIMA[2]

[1]ENERGARID laboratory, faculty of Sciences and Technology
University Tahri Mohammed, P.O.Box 147 route Kenadza Béchar 08000 ALGERIA
[2]Departement of technology, University centre of Naama. Po.Box 66 Naama. Algeria
*Corresponding Author: Mohamed.naima@univ-bechar.dz

Abstract

Nanofluids offer challenging opportunities to enhance the existing thermal processes by altering the fluid and flow characteristics. This paper aims to investigate numerically the double-diffusive convection driven by horizontal thermal and solutal gradients with no-slip wall conditions. The geometry is a square cavity filled with a binary saturated nanofluid in which the vertical walls are maintained at different but uniform and constant temperatures and concentrations. The horizontal walls are assumed to be isolated and impermeable. The system of coupled equations is solved numerically using Finite element code COMSOL multiphysics. The simulation shows that four possible flow cases may present, according to the solutal and thermal contribution on the buoyancy (Adding or opposing buoyancies). The results show that the thermal Rayleigh number promotes clockwise convective flow for the considered cavity configuration. Solutal Rayleigh number promotes anti-clockwise convective flow for opposing buoyancy. The overall flow direction is determined according to the dominance of either thermal or solutal Rayleigh numbers. The convection is more sensitive to the variation of the solutal Rayleigh number in Binary nanofluids and took place at a lower thermal Rayleigh number for adding buoyancies compared to that in ordinary fluids.

Keywords: Binary nanofluid, Comsol, Double diffusion. Heat transfer, Thermosolutal.

1. Introduction

Due to the increase in energy prices and environmental considerations, heat transfer control has become of great importance in most engineering applications. Extensive researches were conducted to develop some techniques to enhance the rate and performance of heat transfer in many industrial applications [1]. According to Tabish Alam [2], those techniques are classified into two main categories: passive and active. Passive methods involve using some fluid additives, geometry improvement, and inserting internal devices to modify the flow patterns. A comprehensive literature review on those passive devices and their wide use in many industrial applications is found in the works of Maradiya et al. [3].

Meanwhile, active techniques employ external power sources such as electric field (Electrohydrodynamic EHD), acoustic or magnetic field (Magnetohydrodynamic MHD), fluid rotation and, fluid vibration to alter the fluid flow characteristics to create the desirable enhancement [4]. Some researchers combine active and passive methods to improve heat transfer performance; others prefer to use passive methods due to their relatively low implementation costs. Rashidi S. [5] published a paper about heat transfer enhancement by combining passive methods, fluid suspensions, and inserts. Compared to the existing techniques to improve heat transfer rates in conventional fluids used as a heat transporting media such as mineral oil, synthetic oil, water, ethylene Glycol, etc., suspension of nanometer-sized particles (10-100 nm) in fluids is found to be a potential in the enhancement of thermal heat conductivity of those named nanofluids [6, 7].

The term nanofluid was first proposed by Choi [8], who claimed that heat transfer could be enhanced by adding those suspended nanoparticles to a fluid. Buongiorno [9] established a system of conservation equations to study the nanofluids taking into account the Brownian and thermophoresis effects. Many authors investigated the presence of nanoparticles in fluids and mixture of fluids. When nanoparticles are added to a binary fluid mixture, it is called a binary nanofluid, and it generates double-diffusive convection due to temperature and concentration differences known as thermosolutal convection. Binary nanofluids can offer significant potential to many engineering applications such as petroleum recovery, electronic component cooling, geophysics, cancer therapy, bioengineering, solar thermal applications, etc.

The presence of nanoparticles alters the flow characteristics and enhances the heat transfer rates. Khanafer et al. [6] confirmed that adding suspended particles enhances heat transfer rates for any value of Grashof number, and this enhancement is proportional to the nanoparticles' volume fraction. Bachir et al. [10] studied the natural convection in a Rayleigh Benard configuration. They showed that the nanofluids volume fraction contributes significantly to the increase of natural convection heat transfer up to 10% volume fraction. Mahmoud SH. [11] recently investigated numerically the effect of nanoparticles volume fraction and nanoparticles size on the conjugated combined convective heat transfer for Al_2O_3 used in a solar collector. He found that the performance is increased by 84.35% with less pressure drop at 2% volume fraction and 25 μm nanoparticles size.

Hussein et al. [12] provided a detailed review of the capability of the nanofluid in enhancing the performance of different types of solar stills. They showed that the water - nanoparticle mixture increases the solar still productivity. Dhinesh et al.

[13] reported that an addition of 25 ppm of Titanium dioxide TiO_2 nanoparticles to Methyl Ester-Diesel blends enhances the break thermal efficiency by 3.60% for a direct injection diesel engine. This Titanium addition results in 14.20% and 17.40% reductions in fuel consumption. Important results also were driven by Elumalai et al. [14] when using a diesel biofuel blend with 150 ppm of Al_2O_3 to drive a direct injection thermal barrier coating engine, the thermal efficiency and in-cylinder pressure were increased. Meanwhile, the fuel consumption and smoke emissions were decreased compared to conventional diesel fuel.

Putra et al. [15] published a study that presented experimental data of the natural convection of Al_2O_3 water-based nanofluid filled in a horizontal cylinder heated from one side and cooled from the other side. A seeming paradoxical result was noticed. The heat transfer rate was declined. They reported that the presence of Al_2O_3 in water base fluid decreases the heat transfer by convection when increasing nanoparticles for a given Rayleigh number. Moreover, Putra et al. [15] showed that natural convection heat transfer is inversely related to the volume fraction of nanoparticles. Kim et al. [16] reported later that the Nusselt number increases by increasing nanoparticles volume fraction for natural convection in nanofluids. Those results are not consistently supported neither by the experimental results of Putra et al. [15] nor by the results of the numerical study done by Elhajjar et al. [17], who investigated the heat transfer numerically in three different nanofluids using new expressions for heat capacity and thermal expansion coefficient in accordance with thermodynamic law rather than those habitually used in literature.

In addition, Rabiei et al. [18] reported that binary nanofluids are eco-advocating and suitable for refrigeration applications [19]. Thermosolutal convection in a binary nanofluid layer in the porous medium was first studied by Kuznetsov and Nield [20]. The complex expression of the Rayleigh number was simplified after that Yadava et al. [21] and Gupta et al.[22] investigated the thermosolutal convection of a binary nanofluid, and they proposed some expressions of the involved parameters used over a wide range of conditions.

It can be seen that there are some gaps in the research field of double convection in binary nanofluids, such as the effect of the location of the reference species on the hot or cold wall. The convection rolls direction and the contribution of thermal and solutal Rayleigh in the overall convection process.

The present paper aims to investigate the onset of a steady-state thermosolutal convection in binary nanofluid filled in a square cavity heated and soluted on vertical sides and subjected to either adding or opposing solutal thermal buoyancy forces. The effect of the positive or negative value of the concentration expansion coefficient and the effect of the location of the considered reference species on the fluid convective motion are studied. The non-dimensional coupled equations describing the problem are solved numerically using the finite element software Comsol Multiphysics.

2. Mathematical formulation

The physical model is a two-dimension square cavity of side length L, filled with a binary nanofluid. The horizontal walls are adiabatic and impermeable. The vertical walls are maintained at constant and different temperatures and concentrations to generate fluid motion ($T_0 > T_1$, $C_0 > C_1$, and $\varphi_0 > \varphi_1$), as shown in Fig. 1.

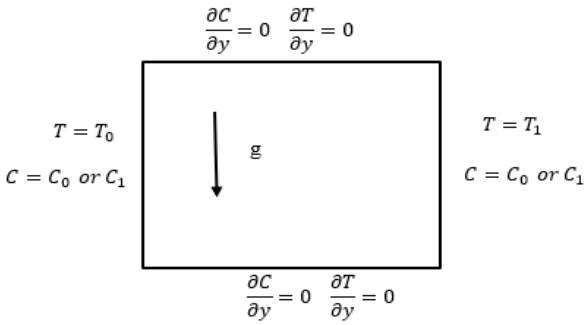

Fig. 1. Geometry of the studied cavity.

The binary nanofluid is assumed to be incompressible; the flow is laminar and with no viscous dissipation. In addition, the Oberbeck–Boussinesq approximation is supposed to be valid, i.e., all the thermophysical properties of the nanofluid are constant except the density in the buoyancy term, which is expressed as a linear function of temperature and concentration as:

$$\rho_f=\rho_r\,[1-\beta_t(T-T_r)-\beta_c(C-C_r] \tag{1}$$

where ρ_r is the reference density of the nanofluid at the reference temperature and reference mass concentration T_r and C_r, respectively. β_t and β_c are the nanofluid thermal expansion and concentration (solutal volumetric) expansion coefficients expressed as follow:

$$\beta_t=-\frac{1}{\rho_r}\frac{\partial\rho}{\partial T} \tag{2}$$

$$\beta_c=-\frac{1}{\rho_r}\frac{\partial\rho}{\partial C} \tag{3}$$

It is worth noting that unlike β_t, which is positive, β_c maybe positive or negative depending on the species choice (light or heavy, respectively). Under the assumption that the nanofluid is stable, no agglomeration or deposition is present (uniform suspension can be achieved by using surfactant or surface charge technology [7]), and no chemical reaction is intended to occur within the system. The governing conservation equations as formulated by Buongiorno [9] as follow:

$$\nabla.V=0 \tag{4}$$

$$\rho\left[\frac{\partial V}{\partial t}+(V.\nabla)V\right]=-\nabla P+[\rho_p\varphi+(1-\varphi)\{\rho_f(1-\beta_t(T-T_1)-\beta_c(C-C_1))\}]\,g+\mu\nabla^2V \tag{5}$$

$$(\rho.Cp)_{nf}\left(\frac{\partial T}{\partial t}+(V.\nabla)T\right)=\lambda\nabla^2T+(\rho.Cp)_p\left[D_B\nabla\varphi\nabla T+\frac{D_T}{T_1}\nabla T\nabla T\right]+(\rho.Cp)_{nf}D_{TC}\nabla^2C \tag{6}$$

$$\frac{\partial C}{\partial t}+(V.\nabla)C=D_s\nabla^2C+D_{CT}\nabla^2T \tag{7}$$

$$\frac{\partial\varphi}{\partial t}+(V.\nabla)\varphi=D_B\nabla^2\varphi+\frac{D_T}{T_1}\nabla^2T \tag{8}$$

where T is the temperature, P is the pressure, $V=(u,v)$ is the fluid velocity, φ is the nanoparticles volume fraction, D_S is the solutal diffusivity, D_B is the Brownian

diffusion coefficient, D_T is the thermophoresis coefficient, D_{CT} is the diffusivity of Soret effect, D_{TC} is the diffusivity of Dufour effect, μ is the fluid viscosity, λ is the thermal conductivity, and Cp is the specific heat capacity. The subscript *nf*, *p*, and *f* refer to nanofluid, nanoparticles, and base fluid, respectively.

To study the hydrodynamic behavior of the fluid, it is convenient to turn the previous equations into a dimensionless form, using the following parameters:

$$x^*, y^* = \frac{(x,y)}{L}; \quad t^* = \frac{t\,\alpha}{L^2}; \quad V^*(u^*, v^*) = \frac{V(u,v)\,L}{\alpha} \quad P^* = \frac{\mu\alpha}{L^2} \tag{9}$$

$$T^* = \frac{T-T_1}{T_0-T_1}; \quad C^* = \frac{C\text{-}C_1}{C_0\text{-}C_1}; \quad \varphi^* = \frac{\varphi\text{-}\varphi_1}{\varphi_0\text{-}\varphi_1}$$

where α is thermal diffusivity given by $\alpha = \lambda/(\rho\, Cp)_f$.

By introducing these dimensionless variables into the system of equations (4-8), and after dropping the superscript asterisks for simplicity reasons, the equations' system becomes:

$$\nabla.V = 0 \tag{10}$$

$$\frac{1}{Pr}\left[\frac{\partial V}{\partial t} + (V.\nabla)V\right] = -\nabla P + \nabla^2 V + \left[-Rm + Ra\,T - Rn\,\varphi + \frac{Rs}{Ls}\,C\right]\hat{e}_y \tag{11}$$

$$\left[\frac{\partial T}{\partial t} + (V.\nabla)T\right] = \nabla^2 T + \frac{N_B}{Le}\nabla\varphi\nabla T + \frac{N_A\ N_B}{Le}\nabla T\,\nabla T + N_{TC}\nabla^2 C \tag{12}$$

$$\frac{\partial C}{\partial t} + (V.\nabla)C = \frac{1}{Ls}\nabla^2 C + N_{CT}\nabla^2 T \tag{13}$$

$$\frac{\partial \varphi}{\partial t} + (V.\nabla)\varphi = \frac{1}{Le}\nabla^2\varphi + \frac{N_A}{Le}\nabla^2 T \tag{2}$$

The new terms appear in the dimensionless form of the governing equations are: Prandtl number $Pr = \mu/(\rho.\alpha)$; Lewis number $Le = \alpha/D_B$; Solutal Lewis number $Ls = \alpha/Ds$; Dufour parameter $N_{TC} = D_{TC}\,\Delta C/(\alpha\,\Delta T)$; Soret parameter $N_{CT} = D_{CT}\,\Delta T/(\alpha\,\Delta C)$; Thermal Rayleigh number $Ra = \rho\, g\, \beta_t \frac{(T_0-T_1)L^3}{\mu\,\alpha}$; Solutal Rayleigh number $Rs = \rho\, g\, \beta_C \frac{(C_0-C_1)L^3}{\mu\, Ds}$; Density Rayleigh number $Rm = [\rho_p\,\varphi_0 + (1\text{-}\varphi_0)\rho]\,gL^3/(\mu\,\alpha)$; Nanoparticles Rayleigh number $Rn = (\rho_p\text{-}\rho)\,(\varphi_0\text{-}\varphi_1)\,gL^3/(\mu\,\alpha)$; Modified diffusivity ratio $N_A = D_T(T_0\text{-}T_1)/(D_B\,T_1(\varphi_0\text{-}\varphi_1))$ and Modified particle density increment $N_B = (\rho\, Cp)_{nf}\Delta\varphi/(\rho\, Cp)_f$.

The momentum equation (11) has been linearized by neglecting all high-order terms involving the product of *T*, *C*, and φ . The linearization is valid only under the assumption of a small temperature gradient in dilute nanofluid with small volume fractions. The boundary conditions of the stated problem in a dimensionless form are:

$$u(0,y) = u(1,y) = u(x,0) = u(x,1) = 0 \tag{35}$$

$$v(0,y) = v(1,y) = v(x,0) = v(x,1) = 0 \tag{46}$$

$$T(0,y) = 1 \quad \forall\, y \in [0-1] \tag{57}$$

$$T(1,y) = 0 \quad \forall\, y \in [0-1] \tag{68}$$

$$\frac{\partial\varphi}{\partial x} + N_A\frac{\partial T}{\partial x} = 0 \ \ at\ y=0\ \ and\ y=1 \tag{79}$$

A mesh sensitivity study was performed to determine the optimum mesh size of the considered geometry. It was found that a mesh consisting of 1492 domain elements and 116 boundary elements is suitable for the present study.

3. Result and discussion.

The numerical solution of the governing equations in the present work is performed using the numerical tool "Comsol Multiphysics" software, which is a cross-platform finite element analysis and solver that allows a fully coupled Multiphysics and single-physics modeling capabilities. It allows conventional physics-based user interfaces and coupled systems of partial differential equations (PDEs). COMSOL provides an Integrated Development Environment (IDE) and unified workflow for electrical, mechanical, fluid, acoustics, and chemical applications. Its Model Builder includes all of the steps in the modeling workflow, from defining geometries, material properties, and the physics that describe specific phenomena to solving and postprocessing models for producing accurate results.

In the first part of this simulation, Comsol is used to treat the problem is treated in the absence of nanoparticles $\varphi = 0$. Since the terms *Rm* and *Rn* will vanish, the problem becomes a typical double diffusivity problem. The instability of the flow and the onset of convection is related to the thermal Rayleigh number *Ra* and the solute Rayleigh number *Rs*. Only those two parameters generate the buoyancy forces. Since the solute Rayleigh *Rs* is positive or negative depending on the fraction (heavy or light) choice and the position of this species (right or left wall), four possible cases can be considered and illustrated in the schematic in Fig. 2.

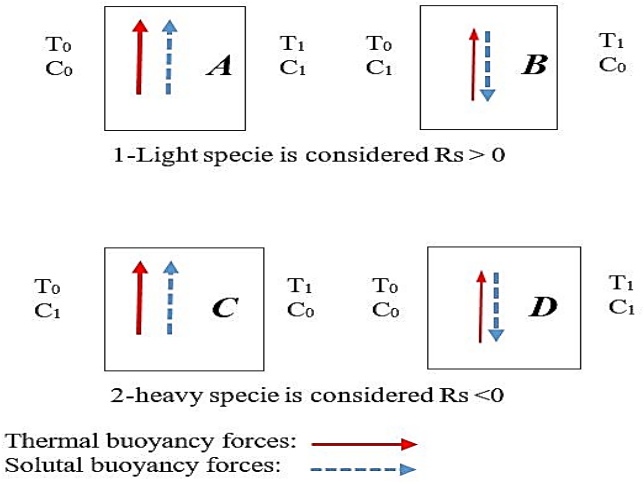

Fig. 2. Studied cavity configurations.

The solutal forces may increase the buoyancy forces and become an added value to the thermal buoyancy forces. By the way, they increase the convection heat transfer and speed up the onset of the convection. This is observed in cases *A* and *C*. In contrast, cases *B* and *D*, where the solutal buoyancy forces oppose the thermal forces, delay the onset of convection, and stabilize the flow.

3.1. Model validation and verification.

To ensure the validation of the model and the accuracy of the calculations used to solve the governing equations, obtained results are compared to available results obtained by Béghein et al. [23]. Assume a Lewis number Ls= α/D_s = 1, i.e., the

mass diffusion of the solute is equal to the thermal diffusion, the Soret and Dufour effects are neglected. For a Prandtl number Pr = 0.7, the simulation of the four cases yields the results shown below.

In Fig. 3. Only thermal buoyancy is considered, with a $Ra = 2 \times 10^4$. At this value, convection occurs, and the flow rolls are clockwise since high temperature is situated on the right side. To better illustrate the effect of solutal Rayleigh number Rs, the absolute values of solutal and thermal Rayleigh numbers are assumed to be equal $Rs = Ra = 10^4$. The simulation results and those obtained by Béghein et al. [21] for the possible four cases are presented below.

In Fig. 4, the light specie is taken as a reference for concentration; therefore, the solutal Rayleigh number is positive, and since the concentration and temperature gradients are in the same direction (from left to right), both solutal and thermal buoyancy will contribute to the convection flow and in the same direction.

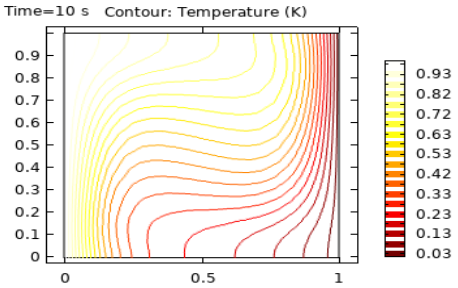

Fig. 3. Thermal contours for $Ra = 2x10^4$ and $Rs = 0$.

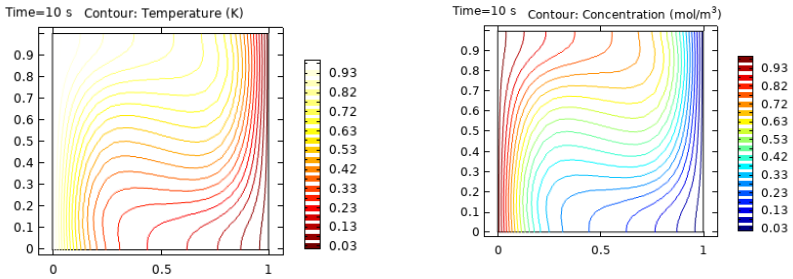

Results obtained by the current model

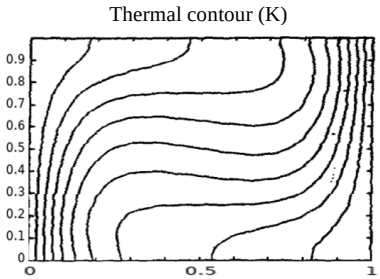

Results obtained by Béghein et al.

Fig. 4. case *A*, $Ra = 10^4$ and $Rs = 10^4$ (increasing buoyancy).

In Fig. 5, the heavy species are considered for concentration; therefore, the solutal Rayleigh number is negative. Since the concentration and temperature gradients are opposite, both solutal and thermal buoyancies will increase the convection flow in the same direction.

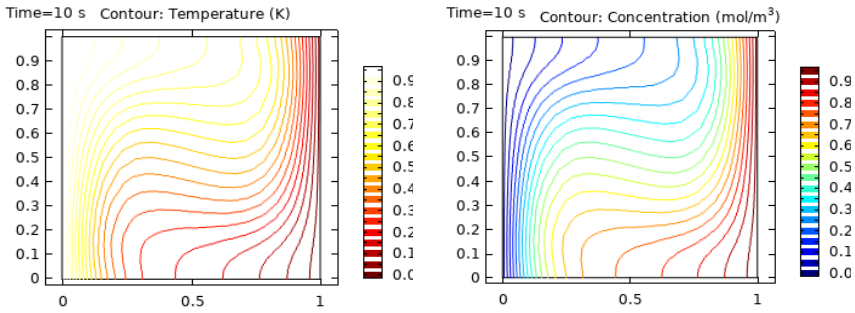

Results obtained by the current model

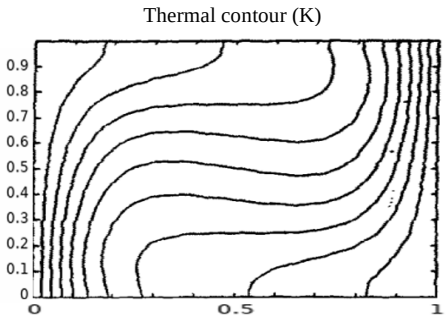

Results obtained by Béghein et al

Fig. 5. case *C*, $Ra = 10^4$ and $Rs = -10^4$ (increasing buoyancy).

One can notice that the obtained results for cases *A* and *C* (Figs. 4 and 5) are similar because they are undergoing the same buoyancy forces, which equal the result of solutal and thermal buoyancy forces. This indeed is the same as that of pure thermal convection illustrated in Fig. 3. with $Ra = 2 \times 10^4$.

These situations are reported by Béghein et al. [23], using a fluid with Pr=0.7 and a pollutant concentration. They found the same thermal isopleths for equal thermal and solutal Rayleigh numbers as used in the present simulation.

In Fig. 6, the light species is taken as the reference species for concentration; therefore, the solutal Rayleigh number is positive. The concentration and temperature gradients are in opposite directions. Solutal and thermal buoyancy will contribute to the flow in opposite directions.

In Fig. 7, the heavy species are considered for concentration; therefore, the solutal Rayleigh number is negative. The concentration and temperature gradients are in the same direction, contributing to the flow in opposite directions. Cases *B* and *D* presented in Figs. 6 and 7 are identical because the thermal and solutal buoyancy forces are opposite. The resulting force has vanished as the *Rs* and *Ra* are equal in absolute values. The flow is stable, and the obtained thermal and concentration isopleths are vertical parallel lines.

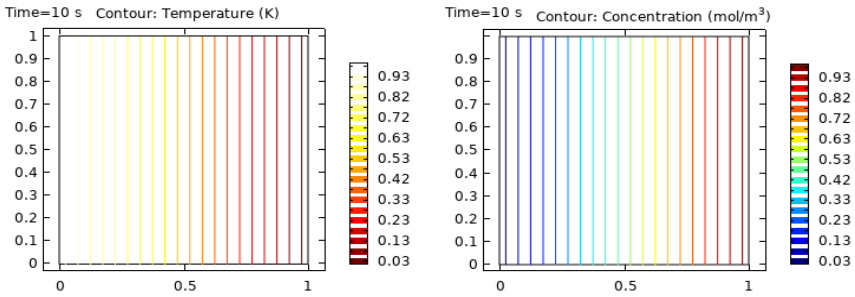

Results obtained by the current model

Thermal contour (K)

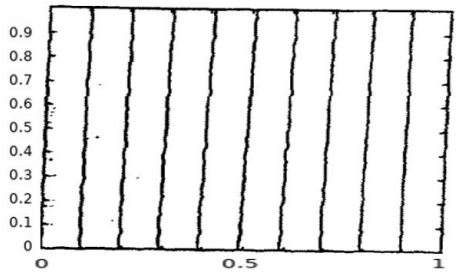

Results obtained by Béghein et al

Fig. 6. case *B*, *Ra* = 10^4 and *Rs* = 10^4 (opposing buoyancies).

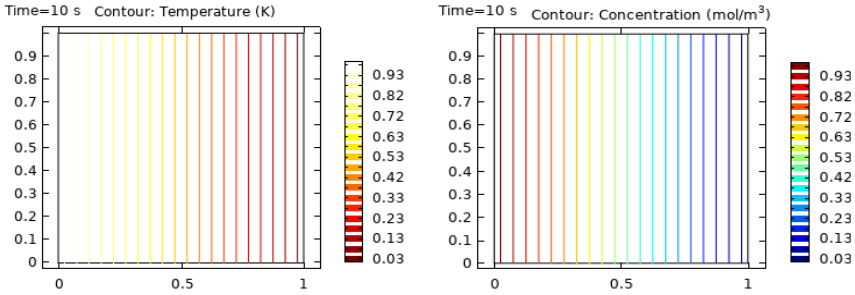

Results obtained by the current model

Thermal contour (K)

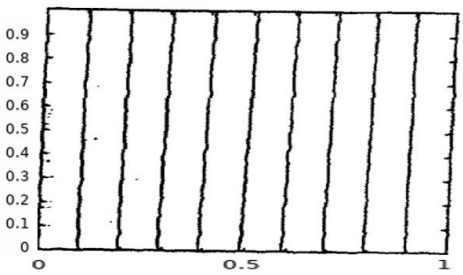

Results obtained by Béghein et al

Fig. 7. case *D*, *Ra* = 10^4 and *Rs* = -10^4 (opposing buoyancies).

The obtained results have the same patterns and are in good agreement with results obtained by Béghein et al. [23] for the thermal contours. Béghein et al. did not plot the results of the concentration Isopleths, but they stated that they would be the same as isothermal contours since the absolute values of *Ra* and *Rs* are assumed equal. The obtained results are also in agreement with those cited in the literature and detailed by Koufi et al. [24] for normal fluid thermosolutal convection.

3.2. Simulation of thermosolutal convection in binary nanofluids.

In the second part of the simulation, a series of parametric sweeps will be conducted to determine the influence of the *Rs* parameter in the convection heat transfer. During the simulation, the values of the nanofluid parameters are calculated using available data published by Yadav et al. [21] and by Sharma et al.[25].

The dimensionless parameters used in equations (10-14) for the simulation of double-diffusive convection in Alumina/water nanofluid are kept constant, as mentioned below in Table 1.

Table 1. Double diffusive Alumina-Water Nanofluid parameters.

Parameter	Value
Lewis Number Ls	2
Nanofluid Lewis number Le	$5x10^3$
Dufour parameter N_{TC}	0.03
Soret parameter N_{CT}	2
Modified Diffusivity ratio N_A	5
Modified Particle density increment N_B	7.5×10^{-4}
Nanoparticles Rayleigh number	0.122

For a constant Rayleigh number *Ra* = 500, the solutal Rayleigh *Rs*' influence is investigated by varying its values as 0, 200, and 500. Notice that the simulations were carried out as mentioned in configuration *A*; the binary nanofluid is heated and soluted from the left side of the cavity. To better emphasize the influence of *Rs* on convection, the temperatures across a vertical cutline that passes through the coordinate *x* = 0.5 are plotted and compared. Below the arc length represents the *y* axis, Fig. 8. illustrates the case for *Rs* = 0.

Figures 9 and 10 show that at *y*=0, the dimensionless temperature goes down as the Rs increases. Meanwhile, at *y*=1, it goes up in S shape mode. This indicates that the convection occurs, and a clockwise roll is formed even at a low thermal Rayleigh number.

The studied cases show that the solutal Rayleigh *Rs* positively contribute to the convective heat transfer as the curve becomes wider and the fluid becomes more unstable. Concentration and temperature gradients are in the same direction (from left to right), which causes an augmenting flow and increase in the buoyancy forces.

The opposing case is also studied where the gradient temperature is from left to right in contrast to the concentration gradient. The investigation is limited to the last case of *Ra* = 500 and *Rs* = 500.

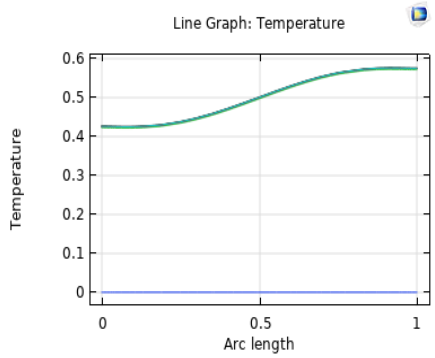

Fig. 8. Temperature line graph (*Ra* = 500; *Rs* = 0).

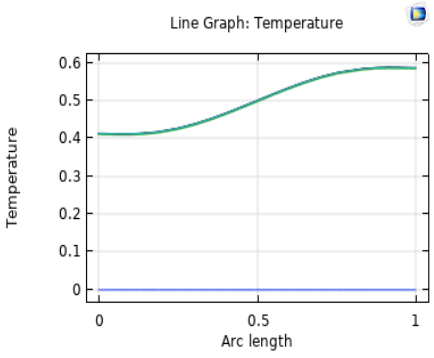

Fig. 9. Temperature line graph (*Ra* = 500; *Rs* = 200).

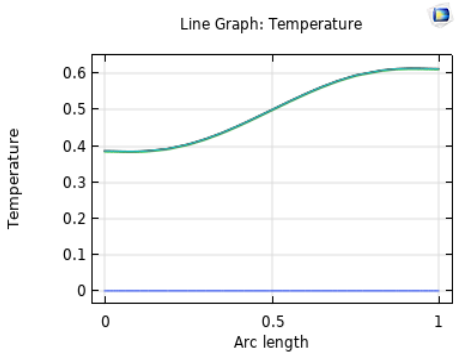

Fig. 10. Temperature line graph (*Ra*=500; *Rs*=500) (Augmenting case).

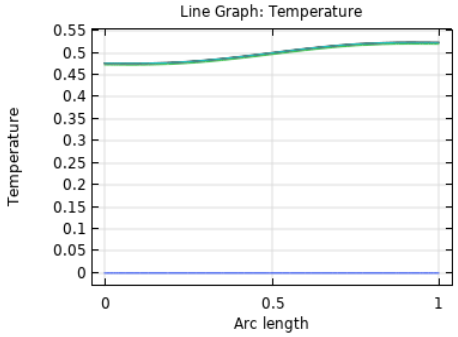

Fig. 11. Temperature line graph (*Ra*=500; *Rs*=500) (Opposite case).

A noticeable remark is that the temperature cutline represented in Fig. 11. is not a straight line $T = 0.5$. The temperature contour in Fig. 12 and concentration in Fig. 13 are not stratified, showing that there is still a slight motion in the clockwise direction for an opposing flow at low *Ra*. This is because Lewis number *Ls* = 2, i.e., the buoyancy forces are not totally opposite. There is a contribution of *Rn*, which belongs to the change in concentration and nanoparticles fraction.

A plot of the dimensionless velocity contours in Fig. 14 shows that the flow occurs at very low velocities near the cavity walls. Five rolls are formed, one at the center of the cavity where the fluid becomes stagnant. The remaining roles are formed next to each wall side. The velocity reaches a maximum value and decreases when going outside the rolls towards the cavity walls to satisfy nonslip conditions at the wall surfaces.

Figure 15 is a representation of the velocity arrows. It indicates that the fluid flow in the convection motion is in the clockwise direction as it consolidates the results of isopleths of temperature and concentration shown in Figs. 12 and 13, respectively.

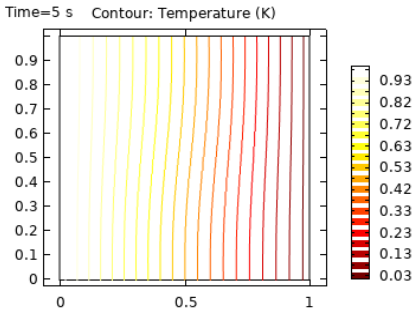

Fig. 12. Temperature isopleths (*Ra* = 500; *Rs* = 500).

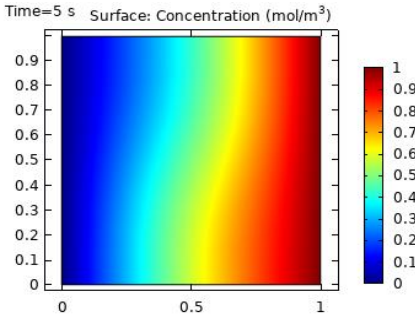

Fig. 13. Concentration isopleths (*Ra* = 500; *Rs* = 500).

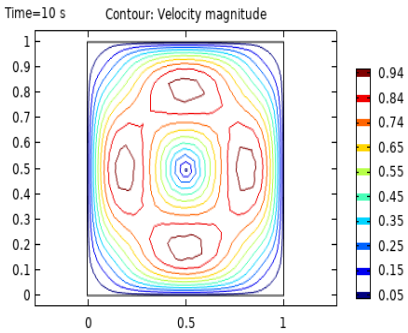

Fig. 14. Velocity contour (*Ra* = 500; *Rs* = 500).

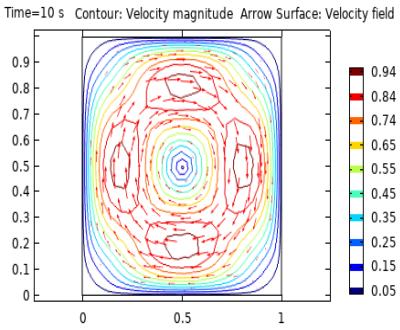

Fig. 15. Velocity direction arrows (*Ra* = 500; *Rs* = 500).

The simulation of other parameters shows that their contribution is not significant in augmenting heat transfer by convection. However, according to the results of linear stability analysis, they still have a considerable role in the delay or speed up of the onset of convection [25].

4. Conclusion

The finite element method (Comsol) is used to investigate the thermosolutal convection in a square cavity filled with a binary nanofluid. A series of simulations were conducted dealing with the problem of convection in the absence of nanoparticles. Lewis number of the species in question equals unity; the thermal buoyancy is kept constant while varying the solutal buoyancy forces.

The second series of simulations on binary nanofluid is performed by varying the solutal Rayleigh number *Rs*. The main conclusions driven from these simulations are:

- The solutal effect increases the buoyancy forces (augmenting flow) when:
  a. The concentration and thermal gradients are in the same direction, and *Rs* is positive (light species is considered).
  b. The solutal gradient opposites thermal gradient and *Rs* is negative (heavier species is considered).

In other possible cases, the solutal effect will decrease the buoyancy (opposing flow) and stabilize the flow.

- In opposing flow, the dominance of thermal buoyancy or solutal buoyancy determines the direction of the flow. Thermal buoyancy promotes a clockwise flow, while solutal buoyancy promotes anti-clockwise flow.
- In a soluted and heated cavity from left with $\beta c>0$ (lighter species is considered), the convection occurs at a relatively low thermal Rayleigh number compared to that in ordinary fluids.
- Convection in a binary nanofluid is more sensitive to the solutal Rayleigh number *Rs* than other parameters.

Nomenclatures

C	Dimensionless concentration
Cp	Specific heat, J. kg^{-1}. K^{-1}
D_B	Brownian diffusion coefficient, m^2.s^{-1}
D_S	Solutal diffusion coefficient, m^2.s^{-1}
D_T	Thermophoretic diffusion coefficient, m^2.s^{-1}
D_{CT}	Diffusivity of Soret type, m^2.s^{-1}
D_{TC}	Diffusivity of Dufour type, m^2.s^{-1}
G	Gravitational acceleration, m.s^{-2}
L	Length of the cavity, m
Le	Thermal nanofluid Lewis number.
Ls	Solutal Lewis number.
N_A	Modified diffusivity ration
N_B	Modified particles density increment
N_{CT}	Soret parameter
N_{TC}	Dufour parameter
P	Dimensionless pressure
Pr	Prandtl number.
Ra	Thermal Rayleigh number.
Rm	Density Rayleigh number
Rn	Nanoparticles Rayleigh number
Rs	Solutal Rayleigh number.
T	dimensionless temperature
T	Dimensionless time
V	Dimensionless velocity
x,y	Coordinate horizontal and vertical directions

Greek symbols

α	Thermal diffusivity, m^2. s-^{1}
β_t	Thermal expansion coefficient, K^{-1}
β_c	Solute volumetric coefficient,
φ	Nanoparticles volume fraction
υ	Kinematic viscosity m^2.s^2
μ	Dynamic viscosity, kg. m^{-1}.s^{-1}
ρ	Density kg.m^{-3}
λ	Thermal conductivity, W.m^{-1}.K^{-1}

Subscripts

P	Nanoparticle
F	Base-fluid
Nf	Nanofluid

References

1. Gugulothu, R.; Reddy, K.V.K.; Somanchi, N.S.; and Adithya, E.L. (2017). A review on enhancement of heat transfer techniques. *Materials Today: Proceedings*, 4, 1051-1056.
2. Alam, T.; and Kim, M.-H. (2018). A comprehensive review on single phase heat transfer enhancement techniques in heat exchanger applications. *Renewable and Sustainable Energy Reviews*, 81, 813-839.
3. Maradiya, C.; Vadher, J.; and Agarwal, R. (2018). The heat transfer enhancement techniques and their thermal performance factor. *Beni-Suef University Journal of Basic and Applied Sciences*, 7, 1-21.
4. Mousa, M.H.; Miljkovic, N.; and Nawaz, K. (2021). Review of heat transfer enhancement techniques for single phase flows. *Renewable and Sustainable Energy Reviews*, 137, 110566.
5. Rashidi, S.; Eskandarian, M.; Mahian, O.; and Poncet, S. (2019). Combination of nanofluid and inserts for heat transfer enhancement. *Journal of Thermal Analysis and Calorimetry*, 135, 437-460.
6. Khanafer, K.; Vafai, K.; and Lightstone, M. (2003). Buoyancy-driven heat transfer enhancement in a two-dimensional enclosure utilizing nanofluids. *International journal of heat and mass transfer*, 46, 3639-3653.
7. Leong, K.Y.; Razali, I.; Ahmad, K.K.; Amer, N.H.; and Akmal, H. (2018). Thermal conductivity characteristic of titanium dioxide water based nanofluids subjected to various types of surfactant. *Journal of Engineering Science and Technology*, 13, 1677-1689.
8. Choi, S.U.; and Eastman, J.A., (1995). Enhancing thermal conductivity of fluids with nanoparticles. Argonne National Lab., IL (United States).
9. Buongiorno, J. (2006). Convective transport in nanofluids. *Journal of Heat Transfer*, 128(3), 240-250.
10. Bachir, G.; Sawli, R.; Fakih, C.; and MOJTABI, A. (2008). Etude du transfert de chaleur en convection naturelle dans les nanofluides. *Congès de la Société Française de Thermique*, 1-6.
11. Mahmoud, M.S. (2021). Numerical investigation of conjugate combined convective heat transfer for internal laminar flow of al2o3/water nanofluid through tube–flat plate solar collector. *Journal of Engineering Science and Technology*, 16, 2378-2393.
12. Hussein, A.K.; Kolsi, L.; Younis, O.; Li, D.; Ali, H.M.; and Afrand, M. (2020). Using of nanotechnology concept to enhance the performance of solar stills-recent advances and overview. *Journal of Engineering Science and Technology*, 15, 3991-4031.
13. Balasubramanian, D.; and Lawrence, K.R. (2019). Influence on the effect of titanium dioxide nanoparticles as an additive with Mimusops elengi methyl ester in a CI engine. *Environmental Science and Pollution Research*, 26, 16493-16502.

14. Elumalai, P.; Nambiraj, M.; Parthasarathy, M.; Balasubramanian, D.; Hariharan, V.; and Jayakar, J. (2021). Experimental investigation to reduce environmental pollutants using biofuel nano-water emulsion in thermal barrier coated engine. *Fuel*, 285, 119200.
15. Putra, N.; Roetzel, W.; and Das, S.K. (2003). Natural convection of nano-fluids. *Heat and mass transfer*, 39, 775-784.
16. Kim, J.; Kang, Y.T.; and Choi, C.K. (2004). Analysis of convective instability and heat transfer characteristics of nanofluids. *Physics of fluids*, 16, 2395-2401.
17. Elhajjar, B.; Bachir, G.; Mojtabi, A.; Fakih, C.; and Charrier-Mojtabi, M.C. (2010). Modeling of Rayleigh–Bénard natural convection heat transfer in nanofluids. *Comptes Rendus Mécanique*, 338, 350-354.
18. Rabiei, F.; Rahimi, A.; and Hadad, M. (2017). Performance improvement of eco-friendly MQL technique by using hybrid nanofluid and ultrasonic-assisted grinding. *The International Journal of Advanced Manufacturing Technology*, 93, 1001-1015.
19. Kasaeipoor, A.; Malekshah, E.H.; and Kolsi, L. (2017). Free convection heat transfer and entropy generation analysis of MWCNT-MgO (15%−85%)/Water nanofluid using Lattice Boltzmann method in cavity with refrigerant solid body-Experimental thermo-physical properties. *Powder Technology*, 322, 9-23.
20. Kuznetsov, A.; and Nield, D. (2010). The onset of double-diffusive nanofluid convection in a layer of a saturated porous medium. *Transport in porous media*, 85, 941-951.
21. Yadav, D.; Agrawal, G.; and Bhargava, R. (2012). The onset of convection in a binary nanofluid saturated porous layer. *International Journal of Theoretical and Applied Multiscale Mechanics*, 2, 198-224.
22. Gupta, U.; Sharma, J.; and Wanchoo, R., (2014). Thermosolutal convection in a horizontal nanofluid layer: introduction of oscillatory motions. 2014 *Recent Advances in Engineering and Computational Sciences* (*RAECS*)IEEE. 1-6.
23. Beghein, C.; Haghighat, F.; and Allard, F. (1992). Numerical study of double-diffusive natural convection in a square cavity. *International Journal of Heat and Mass Transfer*, 35, 833-846.
24. Koufi, L.; Cherif, Y.; Younsi, Z.; and Naji, H. (2019). Double-diffusive natural convection in a mixture-filled cavity with walls' opposite temperatures and concentrations. *Heat Transfer Engineering*, 40, 1268-1285.
25. Sharma, J.; Gupta, U.; and Sharma, V. (2017). Modified model for binary nanofluid convection with initial constant nanoparticle volume fraction. *Journal Of Applied Fluid Mechanics* (*JAFM*), 10, 1387-1395.